Dynamic Confinement Effects in Polymer Blends. A Quasielastic Neutron Scattering Study of the Dynamics of Poly(ethylene oxide) in a Blend with Poly(vinyl acetate)

M. Tyagi,[†] A. Arbe,*[,‡] J. Colmenero,[†,‡,§] B. Frick,[⊥] and J. R. Stewart[⊥]

Donostia International Physics Center, Paseo Manuel de Lardizabal 4, 20018 San Sebastián, Spain; Unidad Física de Materiales (CSIC−UPV/EHU), Apartado 1072, 20080 San Sebastián, Spain; Departamento de Física de Materiales, UPV/EHU, Apartado 1072, 20080 San Sebastián, Spain; and Institut Laue-Langevin, BP 156, 38042 Grenoble Cedex 9, France

Received December 10, 2005; Revised Manuscript Received February 24, 2006

ABSTRACT: Quasielastic neutron scattering combined with deuteration labeling has allowed us to follow selectively the dynamics of the hydrogens of poly(ethylene oxide) (PEO, $T_g \approx 220$ K) in a blend with poly(vinyl acetate) (PVAc, $T_g = 315$ K) (20% PEO/80% PVAc in weight, $T_g^{blend} = 280$ K). Temperatures between $T_g^{blend} - 10$ K and $T_g^{blend} + 120$ K have been explored by backscattering techniques, accessing a dynamical window centered on the nanosecond range and with momentum transfers Q in the inter- and intrachain region. Two essentially different dynamical behaviors have been identified for PEO in the blend: (i) at high temperatures ($\approx T_g^{blend} + 100$ K) the dynamics is not qualitatively different from that of a glass-forming homopolymer (regarding spectral shape and dispersion of the time scales); (ii) close to T_g^{blend}, extremely broad distributions of relaxation times are found that do not depend on Q in the high-Q range, strongly suggesting localized dynamics. Apparently, the slowing down of the motions in the PVAc component toward T_g^{blend} leads to the confinement of PEO dynamics on small length scales. As soon as the dynamics of the more rigid polymer becomes fast enough to allow PEO long-range relaxations ($\approx T_g + 80$ K), the fast component reaches a situation of certain equilibrium, at least for length scales of the order of a nanometer. Our results perfectly agree with those reported for PEO in a blend with poly(methyl methacrylate) [Genix et al. *Phys. Rev. E* **2005**, *72*, 031808]. The confined processes in both "rigid environments" show nearly identical features. In addition, neutron diffraction experiments with polarization analysis indicate that, while blending hardly affects the short-range order of PVAc chains, it leads to larger and more distributed characteristic distances involving PEO segments.

1. Introduction

Recently, the question of dynamical miscibility in thermodynamically miscible polymer blends has attracted increasing interest (see, for instance, the works[1−7] and references therein). This can be formulated as, how is a given dynamical process affected by blending? Can we distinguish each blend component from a dynamical point of view, or do they move similarly when blended? Thanks to extensive experimental work during the past two decades, it is now well established that blending does not appreciably affect fast motions and processes active in the glassy state (at least in absence of strong intermolecular interactions), e.g., methyl group rotations[8−10] or even secondary relaxations.[11−13] On the contrary, segmental and chain dynamics are strongly influenced by the presence of other chains (see, e.g., refs 14−21). Concerning α-relaxation, two main effects of blending have been identified. The selective observation of the dynamic response of one of the two components shows that there is a symmetric broadening of any relaxation function with respect to the homopolymer behavior. This broadening dramatically increases as the temperature decreases toward the average glass transition temperature of the blend T_g^{blend}. On the other hand, two different mean relaxation times are usually observed, each of them corresponding to the dynamics of each of the components modified by blending. This is what is called "dynamic heterogeneity". From a theoretical point of view, two kinds of approaches have been proposed to account for such observations: one is based on the idea that thermally driven concentration fluctuations are responsible for both the broadening and the heterogeneity of the dynamics,[22−24] while in the second one the effect of chain connectivity on the local effective concentration of polymer blends (the so-called self-concentration effect) is considered as the main ingredient.[1,15]

Dynamic heterogeneity is magnified in extremely asymmetric blends from a dynamical point of view, i.e., systems where components display very different glass-transition temperatures T_g. This makes them especially interesting cases. For instance, the dynamics of blends of poly(vinyl methyl ether)/polystyrene (PVME/PS) ($T_g^{PS} - T_g^{PVME} = 123$ K) have been subject of a large number of experimental investigations (see, e.g., refs 11 and 25−27). Recently, the extreme case of poly(ethylene oxide)/poly(methyl methacrylate) (PEO/PMMA) ($T_g^{PMMA} - T_g^{PEO} \approx 200$ K) has also spurred a high level of interest.[9,12,14,28−32] Because of miscibility and PEO crystallization problems, the study of this system is restricted to compositions with less than 30% PEO. In fact, the investigation of the dynamics of the minority component in dilute blends is also very interesting: since this polymer is mainly surrounded by chains of the majority component, the role of intermolecular concentration fluctuations is expected to be less important, and self-concentration effects should contribute increasingly more to the dynamic heterogeneity.[33,34]

The combination of these two ingredients (dynamically extremely asymmetric blends and dilution of the low-T_g component) may lead to the emergence of a new effect: the

[†] Donostia International Physics Center.
[‡] CSIC−UPV/EHU.
[§] UPV/EHU.
[⊥] Institut Laue-Langevin.

10.1021/ma052642i CCC: $33.50
Published on Web 03/23/2006

dynamical confinement of the minority component when approaching the average glass transition of the blend. There, the chain segments of the high-T_g component could be considered as static on the time scale of the segmental motions of the low-T_g component, and the dynamics of the latter would correspond to the motional processes of mobile chains embedded within a more or less frozen environment formed by the high-T_g component. By using dielectric spectroscopy, Loithoir et al.[25] found these confinement effects for PVME in the system PVME/PS with concentrations of PS higher than 50 wt %. A confinement length of about 10 Å was suggested. Hints of this phenomenon in the same system can also be identified in the work by Urakawa et al.[35] On the other hand, NMR studies of PEO in PEO/PMMA in a wide temperature range[28,29] revealed clear deviations from the expected behavior (for instance, predictions in terms of the Lodge and McLeish model[1]) toward T_g^{blend}. By combining neutron scattering measurements and molecular dynamics (MD) simulations in this system, Genix et al.[9] also showed evidence of confinement signatures for PEO dynamics in this blend. The immediate question arising is whether this phenomenon is of a general character.

Unfortunately, the literature on dynamics in diluted polymer blends is not very extensive up to the present date.[9,18,25,28,29,33−37] Watanabe et al.[36] studied the dielectric normal mode of polyisoprene (PI) in diluted blends with oligo- and polybutadiene. In this system, PI is the polymer with higher T_g and thus not susceptible to this effect. Haley and Lodge[37] did not extract the information on the low-T_g component of the system investigated by dynamic viscosity measurements. The recent NMR works of Lutz et al.[33,34] were devoted to the extensive study of the dynamics of either polyisoprene[33] or polystyrene[34] as dilute components in different blends. They did not report any effect associated with confinement. However, as the authors noted, all the studies were performed at temperatures well above the glass transition, where these effects are not expected. This was also the case of the fluorescence anisotropy decay measurements on PI/poly(vinylethylene) by Adams and Adolf.[18] As mentioned above, the expected confinement effects should appear for the low-T_g component in blends of polymers with very different values of the homopolymer glass transition temperatures at temperatures close to the average T_g of the blend. The corroboration of this dynamic confinement phenomenon requires focusing on studies of these characteristics.

With these ideas in mind, in this work we have investigated the dynamics of PEO as diluted component in another blend, namely, with poly(vinyl acetate) (PVAc). In this way, we can also address the question: what is the influence of the embedding rigid polymer on the dynamics of the diluted component? Again in this system the mobilities of the two homopolymers are very different: the glass-transition temperatures differ by about 100 K ($T_g^{PEO} \approx 220$ K, $T_g^{PVAc} = 315$ K). The blend of composition 20% PEO/80% PVAc in weight ($T_g^{blend} = 280$ K) has been studied by quasielastic neutron scattering (QENS), in particular by using a backscattering spectrometer accessing a dynamic range in the nanosecond range and momentum transfer (Q) region covering the typical inter- and intramolecular length scales. By selective deuteration, the scattering from the PVAc component was strongly reduced, and thus the dynamics of PEO hydrogens in the blend could be followed. We have investigated a wide temperature range between $T_g^{blend} - 10$ K and $T_g^{blend} + 120$ K. Special emphasis has been made in the region close to T_g^{blend} to look for indications of confined dynamics for PEO. In addition, we have addressed the influence of blending on the structural properties, in particular on the short-range order of these polymers. By using neutron diffraction with polarization analysis, we have investigated the diffraction pattern of the blend and also of pure PVAc as reference (the structure factor of PEO was already available in the literature[38]).

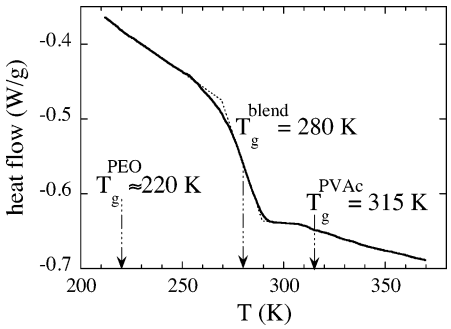

Figure 1. Modulated DSC traces for the dPEO/hPVAc blend sample. The cooling rate was 10 K/min.

After the Experimental Section we first focus on the structural study. The diffraction results are presented and discussed in the same section. Thereafter we move to the investigation of the dynamics. The analysis of the backscattering data is explained and the consequent results are presented in section III. The following section is devoted to the discussion of these dynamical results. Finally, we summarize the outcomes of both the structural and dynamical studies.

2. Experimental Section

A. Samples. The samples investigated in this work are fully protonated poly(vinyl acetate) (hPVAc), fully deuterated poly(vinyl acetate) (dPVAc), fully protonated poly(ethylene oxide) (hPEO), and two blends of PVAc and PEO (20% PEO/80% PVAc in weight): a blend where the PVAc component is deuterated and PEO is protonated (hPEO/dPVAc) and a blend where the PVAc component is protonated and PEO is deuterated (dPEO/hPVAc). Several studies including small-angle neutron scattering (SANS) have shown that PEO and PVAc are miscible over a wide range of temperatures and polymer compositions.[39−48] The molecular weights M_w of the polymers involved are $M_w^{hPVAc} = 217$ kg/mol, $M_w^{dPVAc} = 302$ kg/mol, $M_w^{hPEO} = 43$ kg/mol, and $M_w^{dPEO} = 38$ kg/mol. Polydispersity is close to 1.05 for both PEO samples, while PVAc presents broader distributions, characterized by polydispersities of 1.5 for hPVAc and 2.5 for dPVAc.

The samples were prepared inside flat aluminum containers used for neutron scattering measurements. The thicknesses d were chosen such that the transmission for neutrons would be around 90% to optimize the compromise between good statistics and reduced multiple scattering. In the case of hPVAc and dPVAc ($d = 0.25$ and 1.4 mm, respectively), the required amount of sample was put directly into the sample holder and then heated at 100 °C under vacuum. The blends were prepared in the following way: the two components were dissolved in a common solvent—benzene[49]—for 3 days, followed by slow evaporation of the casting solvent in the sample container at room temperature. The samples were kept at 60 °C under vacuum for 10 days to ensure complete evaporation of the benzene. Thereafter, once heated, they were colorless. The thicknesses were of the order of 0.6 mm for hPEO/dPVAc and 0.3 mm for dPEO/hPVAc.

The homopolymers show T_g values of 315 K (PVAc) and ≈220 K (PEO). The melting point of PEO is about 338 K. The T_gs of the blends were determined by DSC. Figure 1 shows that the glass-transition phenomenon in the blend extends over a wide temperature range of about 30 K. A representative value for T_g^{blend} can be considered in the middle of this wide region, namely 280 K. Both blend samples showed similar calorimetric properties.

B. Neutron Scattering Experiments. The change in energy ($\hbar\omega$) and momentum ($\hbar\vec{Q}$) experienced by the scattered neutrons provides

Table 1. Chemical Formula of the Monomer, Coherent, and Incoherent Cross Sections of the Samples Investigated (in Units of barn/Monomer)[a]

sample	monomer	σ_{coh}	σ_{inc}	$\sigma_{inc}^{H}/\sigma_{tot}$
hPVAc	$C_4H_6O_2$	41.2	478.2	0.92
dPVAc	$C_4D_6O_2$	64.2	12.0	0
hPEO	C_2H_4O	22.4	318.8	0.93
hPEO/dPVAc	$(C_2H_4O)_{0.34}$ $(C_4D_6O_2)_{0.66}$	49.9	111.6	0.64
dPEO/hPVAc	$(C_2D_4O)_{0.31}$ $(C_4H_6O_2)_{0.69}$	40.1	332.4	0.89

[a] The ratio between the incoherent cross section of the hydrogens and the total scattering cross section (coherent and incoherent) is also given.

information on the dynamics and structure of the sample investigated.[50−53] The modulus of the momentum transfer Q is determined by the scattering angle θ and the wavelength of the incoming neutrons λ as $Q = 4\pi \sin(\theta/2)/\lambda$. The measured intensity as a function of Q and $\hbar\omega$ contains incoherent and coherent contributions that are weighted by the corresponding cross sections. The incoherent intensity reveals the incoherent scattering function, $S_{inc}(Q,\omega)$, that is related via Fourier transformations to the intermediate incoherent scattering function, $S_{inc}(Q,t)$, and with the self-part of the Van Hove correlation function, $G_{self}(r,t)$. In the classical limit, $G_{self}(r,t)$ is the probability of a given nucleus being at distance r from the position where it was located at a time t before. Thus, incoherent scattering looks at correlations between the positions of the same nucleus at different times. On the other hand, coherent scattering deals with relative positions of atomic pairs. Its intensity is determined by the coherent differential scattering cross section, which reveals structural features. As we will see below, polarization analysis allows to determine the coherent and incoherent contributions to the scattering.

The neutron scattering cross sections for the different atoms involved in our samples are $\sigma_{inc}^{H} = 79.7$ barn, $\sigma_{coh}^{H} = 1.76$ barn, $\sigma_{inc}^{D} = 2.00$ barn, $\sigma_{coh}^{D} = 5.59$ barn, $\sigma_{inc}^{C} = \sigma_{inc}^{O} = 0$, $\sigma_{coh}^{C} = 5.56$ barn, and $\sigma_{coh}^{O} = 4.23$ barn. Table 1 shows the incoherent and coherent scattering cross sections for all the samples investigated in this work. As one can appreciate, the neutron scattering intensities of fully or partially protonated samples are dominated by the incoherent scattering from the hydrogen atoms, and thus QENS experiments reveal the self-motions of these nuclei.

1. IN16 Measurements. The QENS measurements were carried out by means of the IN16 backscattering (BS) spectrometer at the Institut Laue Langevin (ILL), Grenoble. Using $\lambda = 6.27$ Å, an elastic energy resolution of nearly Gaussian shape is obtained with HWHM = 0.4 μeV. The Q range covered was between 0.19 and 1.9 Å^{-1}. QENS spectra were recorded for the hPEO/dPVAc sample at 270, 290, 350, 375, and 400 K with measuring times of about 8 h. Because of the tendency of PEO to crystallize, the diffraction banks available at IN16—which allow following the diffraction pattern of the sample during the QENS measurements—were of utmost importance. Using these diffraction banks, we could verify the absence of crystallinity in our sample during the measurements. The sample was first measured at 350 and 375 K, well above the melting point. Thereafter it was quenched to 290 K and measured at this temperature and then at 270 K. We made an attempt to record data at 310 K, but after 45 min small peaks were visible in the diffraction pattern, indicating crystallization of the PEO component. Finally, the 400 K spectra were obtained. The resolution function of the spectrometer was determined from the measurement of the sample at 2 K, where the scattering is completely elastic. Additionally, just in order to extend previous BS results[9] on the dynamics of the pure PEO component toward larger Q's, we investigated the hPEO sample at 350 K. The acquired data were corrected for detector efficiency, scattering from the sample container, and absorption using the standard programs available at ILL, thus finally providing the experimental scattering function $S(Q,\omega)$.

2. D7 Measurements. The D7 instrument also at the ILL is a diffuse scattering spectrometer and is capable of three directional polarization analysis. The instrument was used in diffraction mode, where an integration over all possible energy values is performed, and finally one obtains differential scattering cross sections. In an ideal situation, the incoherent part is independent of Q (equal to $\sigma_{inc}/4\pi$), and the coherent part reveals the corresponding partial static structure factor. The two contributions at a fixed Q can be obtained from an experiment with polarized neutrons, since the incoherent scattering arising solely from spin disorder flips the neutron spin with probability 2/3, while coherent scattering leaves the spin unchanged.

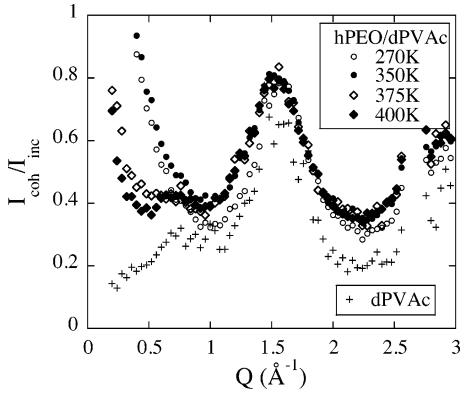

Figure 2. Ratio between the coherent and incoherent intensities scattered by the blend hPEO/dPVAc at different temperatures: 270 K (empty circles), 350 K (full circles), 375 K (empty diamonds), and 400 K (full diamonds). They are compared with the corresponding results for pure dPVAc (pluses) obtained also on D7 at 400 K. The latter have been scaled by 7% of their original values for the purpose of comparison.

The incident wavelength was set to 3.08 Å, enabling a range in Q up to 3.0 Å^{-1}. After quenching from 400 K, the blend sample hPEO/dPVAc was investigated at four temperatures, viz., 270, 350, 375, and 400 K. The other blend dPEO/hPVAc as well as the hPVAc and dPVAc samples were measured only at 400 K. Measuring times were about 2 h. The correction for background scattering was done by measuring the scattering from the empty cell. A vanadium sheet of 0.5 mm thickness was used as an alternative to make the intrinsic incoherent scattering calibration. The multiple scattering may also play a part because consecutive flipping of the neutron spin might restore its original spin and hence lead to an apparent coherent scattering. A standard program available at ILL based on Monte Carlo simulation was used to correct the data for such an effect.

3. Structure Factor

First we investigate the structural information for PVAc in the blend. Figure 2 displays the D7 results obtained from the blend sample where the PEO component is protonated and the PVAc component is deuterated, hPEO/dPVAc. For this sample, the asymptotic value of the ratio between coherent and incoherent scattering for infinite Q is $\sigma_{coh}/\sigma_{inc} = 0.45$ (Table 1), which is consistent with the experimental results. We note that these data will be of utmost importance for the analysis of our BS results, since they provide the Q dependence of the relative fraction of incoherent scattering—mainly due to the PEO component—to the scattered intensity. But apart from this interest, the D7 results offer valuable structural information. Let us first concentrate on the Q range above $\approx$0.7 Å^{-1}. The oscillations of the measured intensities there reflect the average short-range order present in the sample. As the coherent scattering arises mainly from the deuterated PVAc component, constituting 80% of the sample, these peaks basically mirror the structure factor $S(Q)$ of this component in the blend. The comparison with the data obtained at the same temperature for the pure homopolymer melt dPVAc shows that, naturally except for the absolute values, the results are very similar (see Figure 2). This implies that the short-range order in this polymer is

hardly affected by the presence of PEO chains, at least for the concentration here investigated. On the other hand, we observe that the data collected for the blend at 350 K and above collapse in this Q region, while the 270 K results show significantly less intensity on the low-Q side of the main peak. This suggests a predominantly intermolecular nature of this main peak. Turning to the low-Q region, we observe a dramatic increase of the coherent scattering for the blend. This scattering is due to the contrast between deuterated and protonated chains and contains information on the dimensions of the chains and the interaction between them (see, e.g., refs 54 and 55). For the two highest temperatures investigated we observe a strong decrease of this low-Q intensity. This is certainly an interesting effect, but the determination of the chain dimensions in the blend and the deep investigation of this effect will require SANS measurements and is beyond the scope of this article. It will be subject of future work. In any case, the decrease of the low-Q intensity at high temperature allows the resolution of the small structure factor peak centered at about 0.7 $Å^{-1}$ which is also visible in the homopolymer melt. The origin of this prepeak is not clear yet. Polymers with bulky side groups such as PS or PMMA also show a maximum in the structure factor in this range. In these cases, recent MD simulations have shown that this maximum is in fact the true "amorphous halo" of these polymers.[56−58] We do not know whether this could also be the case of PVAc.

Now let us investigate the structural information for PEO in the blend. The results obtained by D7 for the blend sample where the PEO component is deuterated and PVAc is protonated, dPEO/hPVAc, are shown in Figure 3a. At the concentration investigated, the sample contains 2.23 mol of hPVAc per mole of dPEO. Taking into account the cross sections of both polymers, only 20% of the total coherent scattering is due to the dPEO component (see Table 1). This implies that to a large extent the measured coherent scattering reflects the partial structure factor corresponding to the protonated PVAc component (and cross-correlations). For comparison, we have included in the figure the coherent contribution measured for the pure components hPVAc and dPEO[38] weighted by the corresponding fraction of each component in the blend. It is worth noting the extremely broad feature shown by the hPVAc partial structure factor, where no clear peaks but some kind of plateau appears in the usual intermolecular region. Pure PEO, on the contrary, displays a pronounced peak centered at $Q \approx 1.5$ $Å^{-1}$. On the basis of the results obtained for the hPEO/dPVAc sample (Figure 2), we can assume that the short-range order of PVAc is not appreciably altered by blending for this concentration, and we may subtract the hPVAc contributions from the coherent scattering cross section measured for the blend. We note at this point that this is only possible thanks to the *absolute units* provided by neutron diffraction with polarization analysis. In this way we have obtained the data displayed by full squares in Figure 3a. They would approximately correspond to the dPEO structure factor and cross-correlations in the blend. As compared to the pure dPEO structure factor, the main peak present in this "mixed" cross section is clearly broader and shifted to lower Q values, suggesting larger and more widely distributed characteristic distances in the blend or perhaps less dense and stretched chains. Unfortunately, with only the experimental information we have at our disposal, it is not possible to separate the dPEO contributions from those involving pairs of dPEO and hPVAc atoms. This would only be feasible with the help of fully atomistic MD simulations. Therefore, an interpretation of these data is not straightforward. However, it is instructive to compare

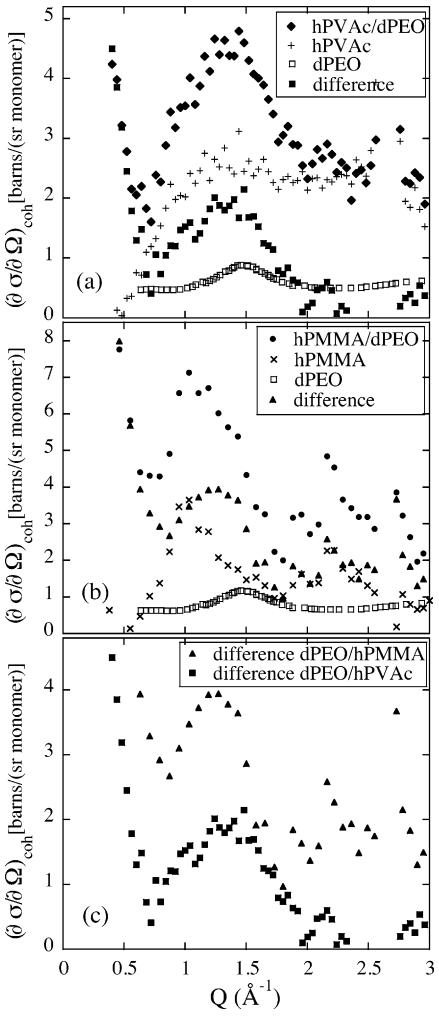

Figure 3. Coherent cross section of the blend dPEO/hPVAc at 400 K measured on D7 (a, full diamonds) and dPEO/hPMMA[9] (b, full circles). The data obtained for the pure components weighted by the corresponding abundances in the samples are also shown: hPVAc multiplied by 0.69 (pluses) and dPEO[38] by 0.55 (empty squares) in (a) and hPMMA multiplied by 0.59 (crosses) and dPEO by 0.73 (empty squares) in (b). The full squares in (a) display the difference between the data of the blend and the contribution of hPVAc and the full up-triangles in (b) the analogous with hPMMA. A direct comparison of the two subtracted curves is shown in (c).

with results on another blend containing dPEO in a low concentration (25%): that with hPMMA. This system was also investigated by neutron diffraction with polarization analysis in a previous study.[9] In an analogous way to Figure 3a, Figure 3b shows the coherent contributions to the scattering of dPEO/hPMMA. In this system, we can see a qualitatively similar effect for the subtracted cross section (see Figure 3b). However, comparing in detail the subtracted cross sections in both cases (Figure 3c), a somewhat broader main peak is observed in the blend with hPVAc. This comparison would suggest a larger effect on the short-range order of the PEO chains when mixed with PVAc rather than with PMMA.

4. Results on the Dynamics

For $Q = 1$ $Å^{-1}$, Figure 4 shows the IN16 spectra obtained for the hPEO/dPVAc sample at different temperatures between 270 and 400 K. With increasing temperature, the intensity of the spectra diminishes in the elastic region while it increases in the quasielastic region. Interestingly, already at 270 K (*below* the blend glass transition) we can observe a large quasielastic contribution. On the other hand, Figure 5 shows the momentum-

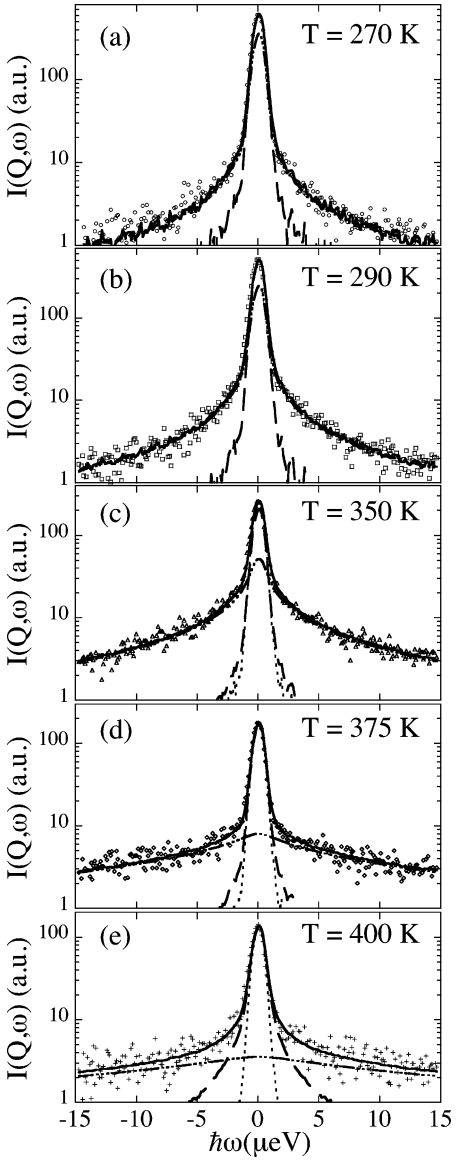

Figure 4. IN16 spectra measured from the hPEO/dPVAc blend at $Q = 0.96$ Å^{-1} and different temperatures: 270 (a), 290 (b), 350 (c), 375 (d), and 400 K (e). The solid lines are fitting curves. The dashed−dotted lines show the contribution of hPEO, modeled through a log−normal distribution of relaxation times. The dashed lines display the slow (KWW) contribution, which in (a) and (b) is just elastic, while in (c), (d), and (e) it is broadened. The instrumental resolution (scaled to match the data in the maximum) is shown as a dotted line for comparison.

transfer dependence of the IN16 spectra for the intermediate temperature investigated, 350 K. As can be seen, with increasing Q the broadening of the spectra becomes more pronounced. This implies some kind of diffusive-like behavior taking place in this temperature range.

A. Analysis. As previously mentioned, the hPEO/dPVAc spectra are dominated by the incoherent contribution from the PEO hydrogens. (The rest of the incoherent scattering, due to PVAc deuterons, can be neglected compared to it; see Table 1.) However, the inspection of Figure 2 shows that, even in the most favorable conditions—close to the minima of the coherent scattering, at $Q \approx 1$ Å^{-1} and at the highest Q's accessed by IN16, $Q \approx 1.8$ Å^{-1}—about 25% of the scattering is coherent. Therefore, to properly describe the IN16 spectra, those non-negligible contributions have to be also taken into account. Let us first qualitatively discuss the nature of such coherent contributions to the scattering. They mainly reveal PVAc pair

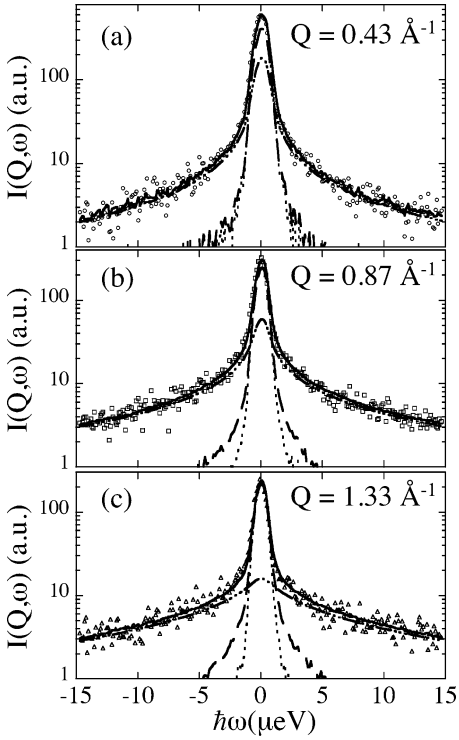

Figure 5. IN16 spectra for hPEO/dPVAc at 350 K and $Q = 0.43$ (a), 0.87 (b), and 1.33 Å^{-1} (c). The solid lines are fitting curves obtained by the addition of the hPEO contribution (log−normal distribution of relaxation times, dashed−dotted lines) and the coherent contribution (KWW functions, dashed lines). The dotted lines show the instrumental resolution scaled to match the data in the maximum.

correlations. In the frequency/temperature window studied, this blend component presents two main processes: methyl group rotations and, above T_g, segmental relaxation. The low-energy barriers for methyl group rotations in PVAc lead to associated time scales that can be accessed by IN16 in the low-temperature range investigated.[59,60] However, motions leading to indistinguishable initial and final atomic configurations—as is the case of methyl group rotations—do not produce coherent quasielastic scattering, and thus this motion is "invisible" to neutrons when the methyl groups are deuterated. On the other hand, being the high-T_g component in the blend, the PVAc segmental dynamics are expected to be slower than those of PEO. In fact, this has been experimentally proven by IN16 measurements on the blend dPEO/hPVAc addressing the hydrogen dynamics of PVAc, which will be subject of a future publication.[61] At low Q values, the coherent scattering reflects other collective phenomena which dynamics would be expected to be also slow. Thus, in the most general case and to a good approximation, we can decompose our spectra into two main contributions:

$$I(Q,\omega) = f_{PEO} S_{inc}^{H,\,PEO/blend}(Q,\omega) + f_{slow} \tilde{S}_{slow}(Q,\omega) \quad (1)$$

The first—and dominant—one is attributed to the incoherent contribution from the PEO hydrogens, and its weight f_{PEO} can be approximated by the incoherent cross section determined from the D7 study. The second one corresponds to the slow contribution associated with the coherent scattering and weighted by f_{slow}, which is obtainable from the coherent cross section measured by D7. The scattering functions $S_{inc}^{H,PEO/blend}(Q,\omega)$ and $\tilde{S}_{slow}(Q,\omega)$ are normalized (total area = unity), and their parametrization requires the choice of a functional form.

It is commonly accepted that for supercooled glass-forming polymers a Kohlrausch−Williams−Watts (KWW) or stretched

exponential function

$$S^{\mathrm{KWW}}(Q,t) = \exp\left[-\left(\frac{t}{\tau_w}\right)^{\beta}\right] \quad (2)$$

is adequate to account for the intermediate scattering function associated with the structural relaxation (equivalently, its Fourier transform describes the scattering function in the frequency domain). Here β is the stretching parameter describing the shape of the relaxation function ($0 < \beta \leq 1$ and close to 0.5 for most polymers[62]), and τ_w the relaxation time which may depend on Q and T.

Our blend system is characterized by a large difference in the glass-transition temperatures of the two components. Above the T_g of the slowest component, PVAc, both polymers are in the supercooled liquid state. There, the presence of the other fast chains does not impose restrictions on the PVAc motions, and this component is in a situation close to that of the metastable equilibrium of the supercooled liquid. Therefore, eq 2 might be used for $\tilde{S}_{\mathrm{slow}}(Q,t)$, and its Fourier transform yields $\tilde{S}_{\mathrm{slow}}(Q,\omega)$. To describe the spectral shape of this component, we used a β value of 0.5, as was determined by BS for the incoherent scattering function of hydrogens in pure PVAc[63] and in this blend.[61] In the low-Q range, we have assumed the same shape for $\tilde{S}_{\mathrm{slow}}(Q,\omega)$ that, in any case, is expected to be elastic or very narrow in our window. The case of the low-T_g component (PEO) is more complicated. At temperatures close to the average glass transition of the blend, this component is in a situation clearly different from that of supercooled liquid state: PEO segments are surrounded by a more or less rigid polymer that is frozen as compared to the PEO characteristic time scale, and therefore it is expected that PVAc imposes a strong confinement on the rapid PEO motions. The phenomenology of these types of confined processes is closer to that of typical glassy dynamics, which is usually characterized by symmetric broadenings of the spectra (like e.g. the secondary (Johari−Goldstein β) relaxation[64,65] or the methyl group rotations[66]). Therefore, under such conditions the KWW function ceases to be valid for describing $S_{\mathrm{inc}}^{\mathrm{H,PEO/blend}}(Q,\omega)$,[9,25] and a log−normal distribution $g(\log\tau)$ of relaxation times seems to be a more appropriate phenomenological function.[9] In the frequency domain the scattering function is built by the superposition of Lorentzian functions

$$S_{\mathrm{inc}}^{\mathrm{H,PEO/blend}}(Q,\omega) = \int_{-\infty}^{+\infty} g(\log\tau)\frac{1}{\pi}\frac{\tau}{1+\omega^2\tau^2}\,\mathrm{d}(\log\tau) \quad (3)$$

where the distribution is characterized by the width σ and the position of its maximum $\log\tau_0$:

$$g(\log\tau) = \frac{1}{\sqrt{2\pi}\sigma}\exp\left[-\frac{(\log\tau - \log\tau_0)^2}{2\sigma^2}\right] \quad (4)$$

Taking into account all the above considerations for the terms involved in eq 1, the experimental IN16 data were fitted with the convolution of this expression with the resolution function. An overall amplitude was also allowed in the fitting procedure.

B. Results of the Analysis. In Figures 4 and 5 we can appreciate the good description achieved for the IN16 data of the blend. Before centering the discussion on the most interesting outcome of this analysis, i.e., the characterization of the PEO dynamics, we briefly comment on the results obtained for the other component, i.e., the slow coherent contribution. We found that an elastic peak gives an adequate account of it at 270 and 290 K (see Figure 4a,b). However, at 350 K and above, this contribution shows quasielastic broadening mainly at high-Q values (see the dashed lines in Figures 4c−e and Figure 5). The characteristic times τ_w obtained for this contribution decrease with increasing temperature and momentum transfer, and they are consistent with the behavior found for the hydrogen motions of PVAc in this blend determined from the QENS study of dPEO/hPVAc,[61] giving support to the analysis performed.

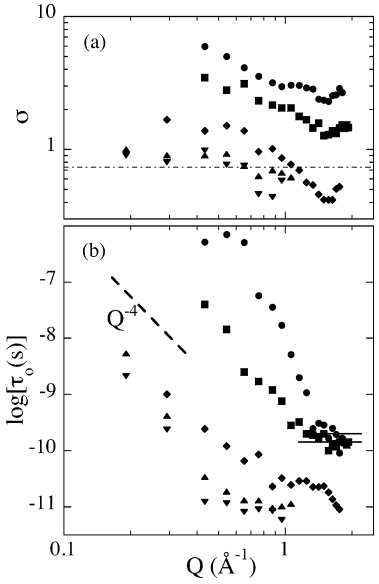

Figure 6. Momentum-transfer dependence of the width σ (a) and the time of the maximum (b) of the log−normal distribution functions describing the hPEO dynamics in the blend. Different symbols correspond to different temperatures: 270 (circles), 290 (squares), 350 (diamonds), 375 (up-triangles), and 400 K (down-triangles). The horizontal dashed−dotted line in (a) shows the width 0.73 (closest distribution to that for a KWW function with $\beta = 0.5$). The horizontal solid lines in (b) indicate the mean value of $\log\tau_0$ above Q^*, $\log\tau^*$.

The parameters characterizing the log−normal distributions used for describing the PEO hydrogen dynamics are displayed in Figure 6 as functions of Q for the different temperatures investigated, and Figure 7 shows some representative examples of the distribution functions. As we can appreciate, the width σ obtained increases with decreasing temperature, and such a tendency is certainly dramatic below room temperature. At the two lowest temperatures, extremely broad functions are revealed. Interestingly enough, for $T \leq 350$ K a tendency for the width σ to increase with decreasing Q value is observed. We note that this behavior is not an artifact of the fitting procedure since it is not possible to properly describe the spectra with Q-independent values for σ. (In that case, the descriptions are deficient, and the characteristic times obtained increase with increasing Q, which makes no sense.) On the other hand, the maximum of $g(\log\tau)$ is shifted toward longer times with decreasing temperature and shows a clear dispersive regime at low Q values. This behavior resembles the in principle expected[9] dependence $\tau_0 \approx Q^{-4}$ for all the temperatures except for the lowest one investigated, 270 K. There, a much steeper dependence is observed. Finally, a certain tendency of the time scales to become flat is found at high Q values. We note that the low intensities together with extremely broad features of the high-Q spectra at the highest temperatures investigated pose difficulties for the precise determination of the width and time scale of the PEO component. In fact, σ and $\log\tau_0$ could not be obtained for $Q > 1$ Å^{-1} at 375 and 400 K. However, this is not the case for the lowest temperatures studied, and thus the flattening of the time scales at 270 and 290 K at high Q should not be an artifact due to this reason. There, the best fits are achieved for

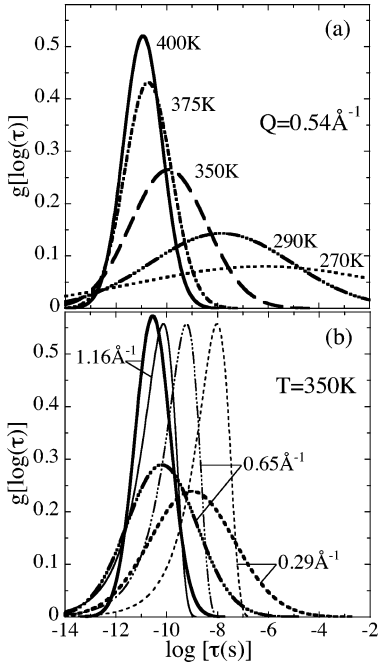

Figure 7. Log−normal distribution functions obtained for the characteristic times of hPEO in the blend at $Q = 0.54$ Å^{-1} and different temperatures (a) and at 350 K and several Q values (b). In (b) the KWW distribution functions predicted by the Lodge and McLeish model are shown as thin lines for comparison.

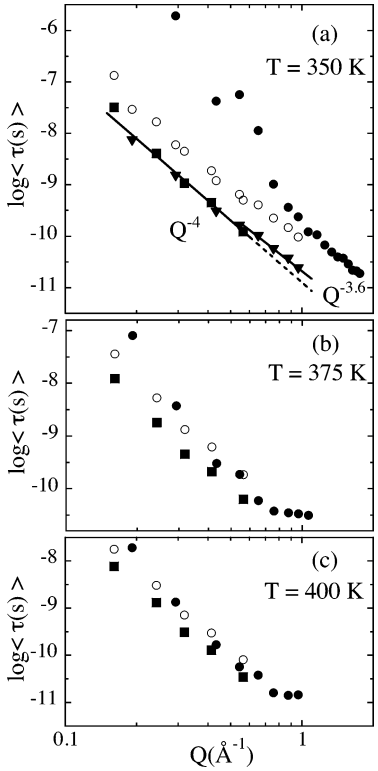

Figure 8. Momentum transfer dependence of the average relaxation time $\langle\tau\rangle$ obtained for pure PEO (full squares from the BS instrument in Jülich[9] and full triangles from IN16) and PEO in the blend (full circles) at 350 (a), 375 (b), and 400 K (c). The empty circles show the Lodge and McLeish prediction starting from the experimental pure PEO data with $\phi_{self}^{PEO} = 0.15$. Solid lines in (a) are power laws $\langle\tau\rangle \propto Q^{-4}$ and $\langle\tau\rangle \propto Q^{-3.6}$, and the dotted line shows the extrapolation of the former one.

power laws between $Q^{-0.25}$ and $Q^{-0.75}$. Moreover, at these temperatures, 290 and 270 K, the uncertainties in the fitting are reduced because the slow component is purely elastic. Finally, we mention that the evaluation of the data collected at 310 K delivers parameter values close to those obtained for 290 K but are subject to a high dispersion due to the bad statistics of the spectra.

5. Discussion

To discuss the effect of blending on PEO dynamics, we first comment on the behavior of the homopolymer melt. A recent BS study[9] in the range $0.16 \leq Q \leq 0.56$ Å^{-1} and $350 \leq T \leq 400$ K has shown that the incoherent scattering function for PEO hydrogens can be well described by the Fourier transform of a KWW function (eq 2) with $\beta = 0.5$ and characteristic times obeying $\tau_w^{PEO} \propto Q^{-4}$. These results perfectly agree with the predictions of the Rouse model.[67,68] The Rouse model describes the Brownian dynamics of a generic linear, ideal Gaussian chain in a polymer melt. In this framework, the conformational entropy of a chain acts as a resource for restoring forces for chain conformations deviating from thermal equilibrium. Toward short length scales this model is limited, since the local chain structure comes into play. Moreover, as a consequence of the rotational potentials, local relaxation mechanisms across the rotational barriers lead to an internal viscosity inducing deviations from Rouse dynamics.[69] The interpretation of PEO findings in light of the Rouse model implies that, contrary to most polymers,[62] the Rouse regime in PEO appears to be valid up to Q values of $Q \approx 0.6$ Å^{-1}. Thus, PEO chains are extremely flexible and show very low internal energy barriers. However, at some length scale deviations from Rouse should be found also for this polymer. The main difficulty in solving this problem is that in the melt PEO dynamics are extremely fast at short length scales, and the quasielastic signal rapidly shifts to higher frequencies than those accessible by the BS window. The gap between 0.56 and 1 Å^{-1} of the BS instrument used in ref 9 prevents exploring Q values higher than 0.56 Å^{-1}. We note that for $Q = 1$ Å^{-1} the signal is already out of the window even for 350 K. Crystallization makes difficult the study at lower temperatures. Trying to address this question, we have performed IN16 measurements on pure protonated PEO at 350 K. This instrument allows exploring Q values in the above-mentioned gap. The data were analyzed in the same way as in ref 9, and in Figure 8a the obtained characteristic times are compared with those reported in that work. In the overlapping region, the results from both instruments perfectly agree. The new data in the high Q range show a slightly weaker slope closer to $\tau_w^{PEO} \propto Q^{-3.6}$. Thus, though subtle, we have found in this Q range the expected deviations from Rouse dynamics. We note, however, that the dispersion of the time scale is still strong, far away from a Q-independent behavior. Finally, a joint fit of the temperature dependence of NMR data[70] and the BS results reported earlier[9] leads to the parameters $C_1 = 8.08$ and $C_2 = 57.7$ in the WLF expression:

$$\log \tau_w = \log \tau_w(T_g) - \frac{C_1(T - T_g)}{C_2 + (T - T_g)} \qquad (5)$$

Next we see what would be the expected behavior of PEO in the blend. The model recently proposed by Lodge and McLeish[1] (LMcL), based on the concept of the "self-concentration", ϕ_{self}, has proven to account for the effect of blending on the component dynamics in a series of systems in the temperature range well above the glass transition of the blend (see as representative references[1,3,4,10,71]). The LMcL model assumes that the mobility of a polymer segment in a blend is determined

by the chemical composition of the region centered in this segment and within one Kuhn length (ℓ_K) of this polymer. Within this volume the concentration of the polymer is enhanced over the bulk concentration due to chain connectivity. In the case of PEO, $\phi_{self}(\ell_K)$ is 0.15, leading to an effective concentration of PEO of 0.32 instead of the average concentration of 0.20. The consequence is a shift of the effective glass transition of this component with respect to the average blend glass transition. From the relative variation of T_g^{blend} predicted by the Fox[72] equation, this shift can be estimated to be about 14 K. The insertion of the effective T_g value (266 K) in eq 5 gives the prediction of this model for the time scales of PEO in the blend. For the three temperatures where experimental data exist for the homopolymer, Figure 8 shows the effect expected for the time scale in this framework. Regarding the spectral shape, no substantial change is predicted.

Now we can compare these predictions with the experimental results. First we focus on the two highest temperatures investigated, 375 and 400 K. There, the width of $g(\log \tau)$ is nearly identical and hardly depends on Q. Also, pure PEO shows a T- and Q-independent shape parameter and so would be the expectation from the LMcL model. A direct comparison of the spectral shape used for describing the dynamics of pure PEO and PEO in the blend is possible through the associated distributions of relaxation times. At least from a mathematical point of view, the KWW function can also be expressed in terms of a superposition of simple exponentials according to an asymmetric distribution of relaxation times $g^{KWW}(\log \tau)$, which for $\beta = 0.5$ has the analytical form

$$g^{KWW}_{\beta=0.5}(\log \tau) = \ln(\sqrt{2\pi})\sqrt{\frac{\tau}{2\tau_w}}\exp\left(-\frac{\tau}{4\tau_w}\right) \qquad (6)$$

For other β values there is not an exact analytical solution for this distribution function, but alternative approaches as that developed in ref 73 can be used. The width σ of the log−normal distribution function most similar to eq 6 ($\beta = 0.5$) is 0.73. As can be seen in Figure 6a, the widths observed for the distributions at the two highest temperatures investigated are rather close to this value. Moreover, below $Q \approx 0.5$ Å^{-1} the time scales in the blend show dispersion, with a slightly stronger dependence than the Q^{-4} found in pure PEO in this range. A direct comparison of the time scales may be done through the average relaxation time $\langle\tau\rangle$ (first moment of the corresponding distribution). This is given by $\log\langle\tau\rangle = \log\ \tau_0 + \sqrt{2\ln(2)}\sigma^2$ for the log−normal distribution and by $\langle\tau\rangle = \Gamma(1/\beta)\tau_w/\beta$ for the KWW function. The results for 375 and 400 K are shown in Figure 8b,c. As can be seen, the average time scales in the blend are slightly shifted to longer times with respect to those in the homopolymer. This effect is reasonably reproduced by the self-concentration model. Thus, we can say that, within the uncertainties, the expectation for a system "in equilibrium" is observed at these high temperatures. In fact, as we have seen that the width of the log−normal distribution is very close to that of the KWW expected for such an equilibrium situation, we may refit the blend spectra with a stretched exponential function ($\beta = 0.5$) for the PEO response. The descriptions produced are also good. The time scales obtained are compared in Figure 9 with those of pure PEO and the expectation from the LMcL model. Then, globally, the experimental results in the blend are closer to the homopolymer times than to the model prediction. The apparently better agreement with the model when comparing the average times (see Figure 8b,c) is due to the fact that for log−normal distributions the average times are located in the region where these functions show their long-time flank. Thus, the conclusion for this temperature region is that neither the spectral shape nor the Q dispersion of PEO in the blend shows a qualitatively different behavior than that typical for a glass-forming polymer well above T_g.

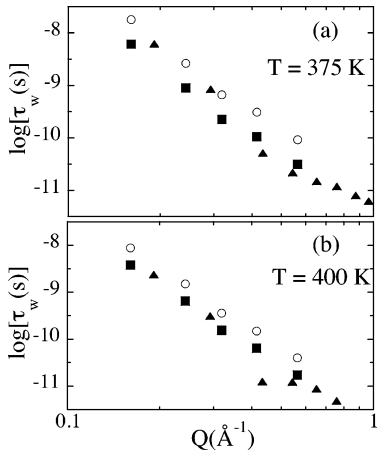

Figure 9. Momentum transfer dependence of the KWW relaxation time τ_w obtained for pure PEO (full squares) and PEO in the blend (full triangles) at 375 (b) and 400 K (c). The empty circles show the Lodge and McLeish prediction starting from the experimental pure PEO data with $\phi_{self}^{PEO} = 0.15$.

At 350 K and below 1 Å^{-1} substantially broader distributions are found in the blend than that expected from the Rouse model and describing the homopolymer results at the same temperature. Moreover, the observed increase of the width with decreasing Q is not compatible anymore with the Rouse model, which predicts constant spectral shapes at intermediate length scales. It is also in contradiction with the expectations of the LMcL model, as clearly shown in Figure 7b. There, model predictions are compared with the obtained distribution functions for three different Q values. While for $Q \approx 1$ Å^{-1} the agreement is rather good, the discrepancies at lower Q values are striking. The change in shape found experimentally is remarkable. In fact, because of this variation of the spectral shape, the average relaxation time $\langle\tau\rangle$ in the blend shows a dramatic increase toward low-Q values (see Figure 8a). This behavior suggests a "rapid" (in space) freezing of the Rouse modes. This means that the bigger the volumes considered, the stronger the slowing down of the dynamics with respect to that expected. Thus, at this temperature (i) we find strong deviations with respect to the self-concentration model predictions (see Figures 7b and 8a) and (ii) we can identify a clear limit for the Rouse motion of PEO in the blend at low Q. This limit could reflect a spatial confinement by the more or less rigid PVAc structure with respect to PEO at this temperature. From the Q value where this deviation from Rouse behavior starts, Q_c, we may define the confinement length scale $\ell_c \approx \pi/Q_c$ of the PEO motion in the blend. For 350 K, $Q_c \approx 0.7$ Å^{-1} leading to $\ell_c \approx 4.5$ Å. At 375 and 400 K hints of this effect—if any—could be seen only at $Q \lesssim 0.2$ Å^{-1} ($\ell_c \gtrsim 16$ Å). This implies that the size of the confined region would increase with increasing temperature; in other words, the confinement would smear out when the rigid surrounding component would move with similar characteristic times.

The behavior described for the 350 K data becomes more pronounced when the temperature approaches the glass transition of the blend. The extremely broad distributions observed at 290 and 270 K and the Q dependences of their widths are not compatible anymore with Rouse-like dynamics. Moreover, as pointed out before, for these low temperatures a flattening of

the time scales is observed at high Q's (see Figure 6b). The value of σ is also Q-independent in this region, and thus even the average time does not show any significant Q dependence. We emphasize that, though in this Q range the Rouse model is not valid anymore, the deviations observed in the homopolymer at 350 K do not give rise to such a flat behavior of the time scales (but to a slightly weaker power law in Q, $\approx Q^{-3.6}$). Therefore, the flattening of $\tau_0^{\mathrm{PEO/blend}}$ at high Q should be caused by the effect of blending. It is well-known that the occurrence of localized processes leads to Q-independent rates as soon as the typical length scale of the motion is smaller than the spatial scale under observation determined by the Q-vector.[50,52] Thus, the behavior found at high Q suggests the occurrence of some processes localized at small length scales for PEO in the blend that are present and detectable by IN16 down to the glass transition of the blend. The Q value where τ_0 becomes flat, Q^* ($Q^* \approx 1.25$ Å^{-1} for 270 and 290 K; see Figure 6b), would reveal a characteristic length scale for the local processes $\ell^* \approx \pi/Q^*$ of $\ell^* \approx 2.5$ Å. Thus, at the lowest temperatures, the length scale of the rapid motions observed should be of the order of $\ell^* \approx 2.5$ Å; beyond, the dynamics is drastically frozen. At 350 K the flattening of the time scale is less evident; since the width of the distribution is also varying with Q, the average time finally shows dispersion in Q also in this region (see Figure 8a) and, in fact, could even be compatible with the expectation for "equilibrium" behavior at $Q \gtrsim 1$ Å^{-1}. This is also the case for the two highest temperatures, where, as already mentioned, the determination of the shape and time scale is rather difficult at high Q values because the signal is very fast for the IN16 window. Thus, for 350 K and above, Q^*—if any—cannot be determined from our results. In any case, we would not expect a clear signature of localized motions due to confinement at the two highest temperatures.

Thus, the results found suggest that with decreasing temperature the dramatic slowing down of the motions in the PVAc component leads to a situation where the PEO dynamics is confined to small length scales. As soon as the dynamics of the more rigid polymer becomes fast enough to allow PEO long-range relaxations (between 350 and 375 K), the fast component reaches a situation of certain equilibrium, at least at length scales of the order of a nanometer. Localized motions of the fast component with characteristic length scales of a few angstroms seem to be active within the confined regions.

Let us focus on the localized motions identified in our system for 270 and 290 K. As we have seen, they show extremely broad distributions of relaxation times. To obtain the characteristic time scale (which we will call τ^*) and width of these distributions, we have averaged the values of $\log \tau_0$ and σ for $Q \geq Q^*$ (see Figure 6). The results are shown in Figure 10 (full squares and shadowed bars). Now we can ask, what is the influence of the matrix on the confined motion? As has been mentioned above, a similar phenomenon was reported for PEO embedded in a PMMA environment.[9] The size of the confined regions at 400 K was estimated to be about 1 nm, i.e., of the same order as here reported, and a Q^* value of about 1 Å^{-1} can be estimated. Figure 10 directly compares the results for the confined motion of PEO in PEO/PMMA below $T_g^{\mathrm{PEO/PMMA}} \approx$ 335 K (calculated from those data in the same way as we did here) with our results for PEO in the blend with PVAc. The agreement between both series of data is impressive. Not only the time scales $\tau^*(T)$ but also the widths of the distributions are perfectly consistent for both systems. Thus, the localized process seems to be an intrinsic feature of the confined PEO chains independently of the nature of the surrounding polymer,

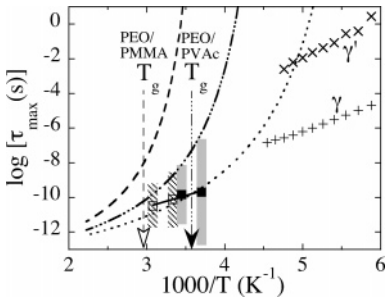

Figure 10. Temperature dependence of the time corresponding to the maximum of the distribution function. The squares show τ^* for PEO in the blend (i.e., the time scale characteristic for the confined motion): solid squares in PEO/PVAc, empty squares in PEO/PMMA.[9] The vertical bars through τ^* indicate the width of the distributions (FWHM). The solid line is an Arrhenius fit of τ^* from PEO in both PMMA and PVAc. The dotted curve corresponds to the time scale of the homopolymer extrapolated to $Q = 1.5$ Å^{-1}. The dashed−dotted curve and the dashed curve are the corresponding predictions of the Lodge and McLeish model for PEO in PEO/PVAc and in PEO/PMMA, respectively. Pluses and crosses are the times for the γ and γ' processes, respectively, as observed for PEO in the blend by dielectric spectroscopy. The vertical arrows indicate the locations of the average glass transitions of both blends.

as soon as the time scale of the segmental motions of the latter become slow enough (see the locations of the respective T_g^{blend} in the figure).

We note that the localized process cannot be identified with the secondary relaxations γ and γ' reported for PEO from dielectric spectroscopy studies.[74] The characteristic time scales of these relaxations are depicted for comparison in Figure 10. They have been obtained by us by isothermal dielectric measurements using a high-resolution Novocontrol alpha analyzer in the frequency range of 10 mHz−3 MHz. Details of the experimental setup and related accuracies can be found elsewhere.[63] The measurements were made on both of the blends (hPEO/dPVAc and dPEO/hPVAc), and there was not any appreciable change between the two. The γ-process has been known to exist in PEO since very early dielectric studies[75] on semicrystalline PEO. At that time it was assigned to the local twisting of main chains in both crystalline and noncrystalline regions. Later on, on the basis of systematic studies of several semicrystalline materials,[76] this process was assigned to the relaxation in fully amorphous regions present in the sample. The origin of γ'-process is not so clear, as was observed recently.[77] In a following study on blends of PEO/PMMA,[74] this process was associated with partially ordered regions of PEO and has been related to the early stages of structural development during polymer crystallization. The excellent matching of characteristic times measured in PEO/PVAc blends with those reported in ref 74 does not contradict this idea. A more extensive discussion on these processes will be addressed elsewhere.[61] We observe that both secondary relaxations are much slower than the localized process identified in the blend by QENS and the activation energies ($E_a = 0.32$ eV for γ and $E_a = 0.52$ eV for γ') are higher than that observed for $\tau^*(T)$. The joint fit of τ^* for PEO in PVAc and PMMA to an Arrhenius law leads to a prefactor of 3.4×10^{-15} s and an activation energy of $E_a = 0.26$ eV (see Figure 10).

The behavior found for PEO close to and below T_g^{blend} resembles the features of a system in an out of equilibrium situation. This becomes evident when we compare the time scales of the confined processes with those characteristic for the "equilibrium situation". In a polymer blend in equilibrium, the expected dynamics is diffusive-like, and we can assume that for each component the time scale can be derived from the

LMcL model. The first feature (diffusive character) implies Q-dependent times in contraposition to those characteristic for the localized motions. Thus, we have to choose a representative Q value to compare equilibrium data with τ^*. This could be in principle any Q within the region where we have found flat behavior for log τ_0. We have taken $Q = 1.5$ Å^{-1} since it is located approximately in the middle of this range. Extrapolating the time scale for pure PEO according to the $Q^{-3.6}$ dependence found for 350 K (Figure 8a), we have calculated the expected WLF for the homopolymer at this Q value (dotted curve in Figure 10). We note that the time scale represented there would also correspond to the maximum of the distribution function, since the maximum of $g^{KWW}_{\beta=0.5}(\log \tau)$ coincides with its average time. Starting from such curve, the LMcL predictions for PEO in PEO/PVAc and in PEO/PMMA have been obtained (dashed−dotted and dashed lines). It becomes clear from this figure that the high-Q behavior of PEO time scales in the blends strongly departs from the "equilibrium" prediction. Interestingly, at low temperatures the maxima of the distribution functions in the blend approach the time scale of the pure polymer. This implies that the application of self-concentration models to this system would require values of $\phi_{self} \approx 1$, which would not fit in these frameworks, in particular within the LMcL model.

We have mentioned in the Introduction that the dynamic confinement effect was also reported for PVME in the system PVME/PS from dielectric spectroscopy measurements.[25,35] In ref 25, a confinement length of about 10 Å was suggested. For PEO we estimate about half of this length scale ($\ell_c \approx 4.5$ Å at 350 K). On the other hand, the activation energy reported for the localized motion of PVME, $E_a = 0.66$ eV, was about 3 times higher than that of the secondary β-relaxation in this polymer. Seemingly, the process active in PEO is more localized and more rapid than that shown by PVME, probably due to its main-chain structure—PVME possesses a large side group.

Finally, we want to emphasize that, though at low temperatures τ^* approximately coincides with the time scale of pure PEO, the associated distributions of relaxation times found in the blend are extremely broad. These distributions contain times similar to those in the pure polymer as well as those times expected from the LMcL model in the case of PEO/PVAc. In fact, here we have used a minimal model to describe the dynamics of PEO in the blend, giving to account for the different phenomenology expected in the out of equilibrium situation. For example, the CONTIN analysis of the MD simulation data of PEO in PMMA[9] revealed a bimodal distribution for PEO segmental dynamics. Also, a bimodal function was used for describing the NMR results on the PEO dynamics in PMMA.[29] The need to employ this kind of function became imperative when the NMR spin−lattice relaxation data previously reported in ref 28 were extended toward lower temperatures with NMR solid echo results. Bimodal distributions are also predicted in the framework of concentration fluctuations models.[24] On the other hand, also recent simulations of dilute model blends of "bead−spring" chains show that the functional form of the scattering function might, in fact, be rather unusual and close to a logarithmic decay with no single time scale associated.[78] Unfortunately, our neutron scattering study does not allow an analysis in terms of bimodal distributions or discriminate between other more complex functions. However, it demonstrates beyond reasonable doubt that PEO dynamics in the blend does not follow the expected equilibrium behavior when approaching the average glass transition and confirms the previous results obtained for PEO in a PEO/PMMA blend.[9]

6. Summary and Concluding Remarks

This work has focused on the structural and dynamical properties of the blend poly(ethylene oxide)/poly(vinyl acetate) in a composition of 20%/80% in weight. The study of the short-range ordered structure has been realized by neutron diffraction with polarization analysis combined with deuteration labeling. Also, deuteration labeling has allowed to selectively investigate the dynamics of the low-T_g component, PEO, at temperatures above and below the average glass transition of the blend. With the backscattering spectrometer used we have accessed time scales of the order of a nanosecond and Q values roughly between 0.2 and 2 Å^{-1}. The studies have been extended to the homopolymers when required for comparison. The results obtained can be summarized as follows:

A. Structure. (1) We have presented for the first time results of neutron diffraction with polarization analysis on the homopolymer PVAc. A prepeak at $Q \approx 0.7$ Å^{-1} and a main peak at $Q \approx 1.4$ Å^{-1} are the main features of the structure factor $S(Q)$ obtained from the fully deuterated sample. In contrast, the partial structure factor revealed by the fully protonated sample is extremely broad with no clear peak structure in the usual intermolecular range.

(2) The short-range order of PVAc chains is hardly affected by the presence of PEO (at least for the concentration here investigated).

(3) Experimentally, it is impossible to isolate completely the structure factor of PEO in the blend. The results suggest larger and more distributed characteristic distances in the blend or perhaps less dense and stretched chains. A comparison with structural results on the blend PEO/PMMA indicates a larger effect on the short-range order of PEO when mixed with PVAc than with PMMA.

(4) Future work involving SANS measurements on this system is planned to determine the chain dimensions for both components and their interaction, as was done for PEO/PMMA.[79,80] Such a study might allow to understand the temperature dependence observed for the coherent scattering in the low-Q range.

B. Dynamics. (1) An extension of the study of pure PEO dynamics toward high-Q values has revealed deviations from Rouse behavior close to $Q \approx 0.5$ Å^{-1}.

(2) Focusing now on the PEO dynamics in the blend, we have reported clear evidence of dynamical processes detectable in the nanosecond window even 10 K below the average glass transition of the blend, T_g^{blend}.

(3) Close to T_g^{blend}, the incoherent scattering function of PEO hydrogens shows an extremely broad feature. Distributions of relaxation times extending over many decades have to be used to describe the spectra. The observation of Q-independent distributions at $Q \gtrsim 1.25$ Å^{-1} strongly suggests the localized character of the observed dynamics. The extent of the motions is of about 2.5 Å. The dramatic increase of the characteristic time toward lower Q values could be interpreted as due to the freezing of the large-scale motions for PEO chains.

(4) At high temperatures (375 and 400 K, i.e., about 100 K above T_g^{blend}) the PEO behavior is rather close to that expected for the low-T_g component of a regular miscible blend. The associated distributions of relaxation times have widths close to those observed in a polymer melt and also the dispersion of the characteristic times. The absolute values of these time scales are slightly faster than those predicted by the Lodge and McLeish model, closer to those measured or extrapolated for the pure homopolymer. Thus, it can be concluded that in such temperature range the PEO behavior is more or less "standard",

in the sense that it is not very different from that of a glass-forming homopolymer.

(5) It is around 350 K (70 K above T_g^{blend}) where the crossover between both *qualitatively different* dynamical regimes takes place. This manifests itself through deviations from Rouse dynamics below ≈ 0.7 Å^{-1} with respect to both the spectral shape and the Q dependence of the average times. The length scale where the dynamic slowing down manifests itself is of about 5 Å at this temperature.

(6) These observations are compatible with the following scenario: the dramatic slowing down of the motions in the PVAc component toward T_g^{blend} leads to the confinement of PEO dynamics to small spatial scales where rapid localized processes with motional amplitudes of ≈ 2.5 Å occur. As soon as the dynamics of the more rigid component become fast enough to allow PEO long-range relaxations (between 350 and 375 K), the fast component reaches a situation of certain equilibrium, at least for length scales of the order of a nanometer.

(7) These results agree perfectly with those reported for PEO in the blend PEO/PMMA (25%/75%).[9] The confined processes in both rigid polymers show nearly identical features.

(8) The activation energy of the confined motions is of about 0.26 eV, much lower than those shown by the secondary relaxations in this system. Thus, the observed phenomenon cannot be identified with those processes.

(9) Extensions of this kind of study of the low-T_g component dynamics close to T_g^{blend} to other systems displaying a large difference in T_g values for the two components would be desirable to establish the generalization of this phenomenon of dynamic confinement in miscible blends.

Acknowledgment. This research project has been supported by the European Commission NoE SoftComp, Contract NMP3-CT-2004-502235. A.A. and J.C. acknowledge support from the projects MAT2004-01017 and 9/UPV00206.215-13568/2001.

References and Notes

(1) Lodge, T. P.; McLeish, T. C. B. *Macromolecules* **2000**, *33*, 5278.
(2) Leroy, E.; Alegría, A.; Colmenero, J. *Macromolecules* **2003**, *36*, 7280.
(3) Hirose, Y.; Urakawa, O.; Adachi, K. *Macromolecules* **2003**, *36*, 3699.
(4) He, Y.; Lutz, T. R.; Ediger, M. D. *J. Chem. Phys.* **2003**, *119*, 9956.
(5) Kant, R.; Kumar, S. K.; Colby, R. H. *Macromolecules* **2003**, *36*, 10087.
(6) Colby, R. H.; Lipson, J. E. G. *Macromolecules* **2005**, *38*, 4919.
(7) Krygier, E.; Lin, G.; Mendes, J.; Mukandela, G.; Azar, D.; Jones, A. A.; Pathak, J. A.; Colby, R. H.; Kumar, S. K.; Floudas, G.; Krishnamoorti, R.; Faust, R. *Macromolecules* **2005**, *38*, 7721.
(8) Mukhopadhyay, R.; Alegría, A.; Colmenero, J.; Frick, B. *J. Non-Cryst. Solids* **1998**, *235*−*237*, 233.
(9) Genix, A.-C.; Arbe, A.; Alvarez, F.; Colmenero, J.; Willner, L.; Richter, D. *Phys. Rev. E* **2005**, *72*, 031808.
(10) Pérez Aparicio, R.; Arbe, A.; Colmenero, J.; Schweika, W.; Richter, D.; Fetters, L. J. *Macromolecules*, in press.
(11) Cendoya, I.; Alegría, A.; Alberdi, J. M.; Colmenero, J.; Grimm, H.; Richter, D.; Frick, B. *Macromolecules* **1999**, *32*, 4065.
(12) Dionísio, M.; Fernandes, A. C.; Mano, J. F.; Correia, N. T.; Sousa, R. C. *Macromolecules* **2000**, *33*, 1002.
(13) Arbe, A.; Alegría, A.; Colmenero, J.; Hoffmann, S.; Willner, L.; Richter, D. *Macromolecules* **1999**, *32*, 7572.
(14) Colby, R. H. *Polymer* **1989**, *30*, 1275.
(15) Chung, G.-C.; Kornfield, J. A.; Smith, S. D. *Macromolecules* **1994**, *27*, 5729.
(16) Arendt, B. H.; Kannan, R. M.; Zewail, M.; Kornfield, J. A.; Smith, S. D. *Rheol. Acta* **1994**, *33*, 322.
(17) Arendt, B. H.; Krishnamoorti, R.; Kornfield, J. A.; Smith, S. D. *Macromolecules* **1997**, *30*, 1127.
(18) Adams, S.; Adolf, D. B. *Macromolecules* **1999**, *32*, 3136.
(19) Hoffmann, S.; Willner, L.; Richter, D.; Arbe, A.; Colmenero, J.; Farago, B. *Phys. Rev. Lett.* **2000**, *85*, 772.
(20) Yang, X.; Halasa, A.; Hsu, W.-L.; Wang, S.-Q. *Macromolecules* **2001**, *34*, 8532.
(21) Min, B.; Qiu, X.; Ediger, M. D.; Pitsikalis, M.; Hadjichristidis, N. *Macromolecules* **2001**, *34*, 4466.
(22) Zetsche, A.; Fischer, E. W. *Acta Polym.* **1994**, *45*, 168.
(23) Katana, G.; Fischer, E. W.; Hack, T.; Abetz, V.; Kremer, F. *Macromolecules* **1995**, *28*, 2714.
(24) Kumar, S. K.; Colby, R. H.; Anastasiadis, S. H.; Fytas, G. *J. Chem. Phys.* **1996**, *105*, 3777.
(25) Lorthioir, C.; Alegría, A.; Colmenero, *Phys. Rev. E* **2003**, *68*, 031805.
(26) Takegoshi, K.; Hikichi, K. *J. Chem. Phys.* **1991**, *94*, 3200.
(27) LeMenestrel, C.; Kenwright, A. M.; Sergot, P.; Lauprêtre, F.; Monnerie, L. *Macromolecules* **1992**, *25*, 3020.
(28) Lutz, T. R.; He, Y. Y.; Ediger, M. D.; Cao, H. H.; Lin, G. X.; Jones, A. A. *Macromolecules* **2003**, *36*, 1724.
(29) Cao, H.; Lin, G.; Jones, A. A. *J. Polym. Sci., Part B: Polym. Phys.* **2005**, *43*, 2433.
(30) Zawada, J. A.; Ylitalo, C. M.; Fuller, G. G.; Colby, R. H.; Long, T. E. *Macromolecules* **1992**, *25*, 2896.
(31) García Sakai, V.; Chen, C.; Maranas, J. K.; Chowdhuri, Z. *Macromolecules* **2004**, *37*, 9975.
(32) Farago, B.; Chen, C.; Maranas, J. K.; Kamath, S.; Colby, R. H.; Pasquale, A. J.; Long, T. E. *Phys. Rev. E* **2005**, *72*, 031809.
(33) Lutz, T. R.; He, Y. Y.; Ediger, M. D.; Pistsikalis, M.; Hadjichistidis, N. *Macromolecules* **2004**, *37*, 6440.
(34) Lutz, T. R.; He, Y. Y.; Ediger, M. D. *Macromolecules* **2005**, *38*, 9826.
(35) Urakawa, O.; Sugihara, T.; Adachi, K. *Polym. Appl. (Jpn.)* **2002**, *51*, 10.
(36) Watanabe, H.; Urakawa, O.; Yamada, H.; Yao, M. L. *Macromolecules* **1996**, *29*, 755.
(37) Haley, J. C.; Lodge, T. P. *Colloid Polym. Sci.* **2004**, *282*, 793.
(38) Johnson, J. A.; Saboungi, M.-L.; Price, D. L.; Ansell, S.; Russell, T. P.; Halley, J. W.; Nielsen, B. *J. Chem. Phys.* **1998**, *109*, 7005.
(39) Martuscelli, E.; Silvestre, C.; Gismondi, C. *Makromol. Chem.* **1985**, *186*, 2161.
(40) Martuscelli, E.; Vicini, L.; Seves, A. *Makromol. Chem.* **1987**, *188*, 607.
(41) Silvestre, C.; Karasz, F. E.; Macknight, W.; Martuscelli, E. *Eur. Polym. J.* **1987**, *23*, 745.
(42) Kalfoglou, N. K.; Soyiropoulou, D. D.; Margaritis, A. G. *Eur. Polym. J.* **1988**, *24*, 389.
(43) Addonozio, M. L.; Martuscelli, E.; Silvestre, C. *J. Polym. Mater.* **1990**, *7*, 63.
(44) Han, C. D.; Chung, H. S.; Kim, J. K. *Polymer* **1992**, *33*, 546.
(45) Yin, J.; Alfonso, G. C.; Turturro, A.; Pedemonte, E. *Polymer* **1993**, *34*, 1465.
(46) Talibuddin, S.; Wu, L. Runt, J.; Lin, J. S. *Macromolecules* **1996**, *29*, 7527.
(47) Chen, X.; Yin, J.; Alfonso, G. C.; Pedemonte, E.; Turturro, A.; Gattiglia, E. *Polymer* **1998**, *39*, 4929.
(48) Huang, C.-I.; Chen, J.-R. *J. Polym. Sci., Part B: Polym. Phys.* **2001**, *39*, 2705.
(49) Wu, W. B.; Chiu, W. Y.; Liau, W. B. *J. Appl. Polym. Sci.* **1997**, *64*, 441.
(50) Springer, T. *Quasielastic Neutron Scattering for the Investigation of Diffusive Motions in Solids, Liquids*; Springer Tracts in Modern Physics; Springer-Verlag: Berlin, 1972; Vol. 64.
(51) Lovesey, S. W. *Theory of Neutron Scattering from Condensed Matter*; Clarendon Press: Oxford, 1984.
(52) Bée, M. *Quasielastic Neutron Scattering;* Adam Hilger: Bristol, 1988.
(53) Squires, G. L. *Introducction to the Theory of Thermal Neutron Scattering*; Dover Publication: New York, 1996.
(54) Higgins, J. S.; Benoit, H. C. *Polymers and Neutron Scattering*; Oxford University Press: Oxford, 1994.
(55) Wignall, G. D.; Melnichenko, Y. B. *Rep. Prog. Phys.* **2005**, *68*, 1761.
(56) Ayyagari, C.; Bedrov, D.; Smith, G. D. *Macromolecules* **2000**, *33*, 6194.
(57) Iradi, I.; Alvarez, F.; Colmenero, J.; Arbe, A. *Physica B* **2004**, *350*, e881.
(58) Genix, A.-C.; Arbe, A.; Alvarez, F.; Colmenero, J.; Schweika, W.; Richter, D. *Macromolecules*, submitted for publication.
(59) Colmenero, J.; Mukhopadhyay, R.; Alegría, A.; Frick, B. *Phys. Rev. Lett.* **1998**, *80*, 2350.
(60) Mukhopadhyay, R.; Alegría, A.; Colmenero, J.; Frick, B. *Macromolecules* **1998**, *31*, 3985.
(61) Tyagi, M.; et al., to be published.
(62) Richter, D.; Monkenbusch, M.; Arbe, A.; Colmenero, J. *Neutron Spin*−*Echo Investigations on Polymer Dynamics;* Adv. Polym. Sci. Vol. 174; Springer-Verlag: Berlin, 2005.
(63) Tyagi, M.; Alegría, A.; Colmenero, J. *J. Chem. Phys.* **2005**, *122*, 244909.
(64) McCrum, N. G.; Read, B. E.; Williams, G. *Anelastic, Dielectric Effects in Polymeric Solids*; Wiley: London, 1967.
(65) *Broad Band Dielectric Spectroscopy*; Kremer, F., Schnhals, A., Eds.; Springer-Verlag: Heidelberg, 2002.
(66) Colmenero, J.; Moreno, A.; Alegría, A. *Prog. Polym. Sci.* **2005**, *30*, 1147.

(67) Rouse, P. E., Jr. *J. Chem. Phys.* **1953**, *21*, 1272.
(68) Doi M.; Edwards, S. F. *The Theory of Polymer Dynamics*; Clarendon Press: Oxford, 1986.
(69) Allegra, G.; Ganazzoli, F. *Adv. Chem. Phys.* **1989**, *75*.
(70) Lartigue, C.; Guillermo, A.; Cohen-Addad, J. P. *J. Polym. Sci., Part B: Polym. Phys.* **1997**, *35*, 1095.
(71) Haley, J. C.; Lodge, T. P.; He, Y.; Ediger, M. D.; von Meerwall, E. D.; Mijovic, J. *Macromolecules* **2003**, *36*, 6142.
(72) Fox, T. G. *Bull. Am. Phys. Soc.* **1956**, *1*, 123.
(73) Gómez, D.; Alegría, A. *J. Non-Cryst. Solids* **2001**, *287*, 246.
(74) Jin X.; Zhang, S.; Runt, J. *Macromolecules* **2004**, *37*, 8110.
(75) Ishida, Y.; Matsuo, M.; Takayanagi, M. *J. Polym. Sci., Part B* **1965**, *3*, 321.
(76) Boyd, R. H. *Polymer* **1985**, *26*, 323.
(77) Jin, X.; Zhang, S.; Runt, J. *Polymer* **2002**, *43*, 6247.
(78) Moreno, A. J.; Colmenero, J. *J. Chem. Phys.*, submitted for publication.
(79) Lefebvre, J.-M. R.; Porter, R. S.; Wignall, G. D. *Polym. Eng. Sci.* **1987**, *27*, 433.
(80) Ito, H.; Russell, T. P.; Wignall, G. D. *Macromolecules* **1987**, *20*, 2213.

MA052642I